




# Enhanced Efficacy of Photodynamic Therapy by Coupling a Cell-Penetrating Peptide with Methylene Blue

This article was published in the following Dove Press journal:  
*International Journal of Nanomedicine*

Jinhui Ser <sup>1,\*</sup>

Ji Yeon Lee <sup>2,\*</sup>

Yong Ho Kim <sup>3</sup>

Hoonsung Cho <sup>1</sup>

<sup>1</sup>School of Materials Science & Engineering, Chonnam National University, Gwangju 61186, Republic of Korea; <sup>2</sup>Department of Anesthesiology and Pain Medicine, Gachon University, Gil Medical Center, Incheon 21565, Republic of Korea; <sup>3</sup>Gachon Pain Center and Department of Physiology, College of Medicine, Gachon University, Incheon 21999, Republic of Korea

\*These authors contributed equally to this work

**Introduction:** Photodynamic therapy (PDT), which induces tissue damage by exposing tissue to a specific wavelength of light in the presence of a photosensitizer and oxygen, is a promising alternative treatment that could be used as an adjunct to chemotherapy and surgery in oncology. Cell-penetrating peptides (CPPs) with high arginine content, such as protamine, have membrane translocation and lysosome localization activities. They have been used in an extensive range of drug delivery applications.

**Methods:** We conjugated cell-penetrating peptides (CPPs) with methylene blue (MB) and then purification by FPLC. Synthesis structure was characterized by the absorbance spectrum, FPLC, MALDI-TOF, and then evaluated cell viability by cytotoxicity assay after photodynamic therapy (PDT) assay. An uptake imaging assay was used to determine the sites of MB and MB-Pro in subcellular compartments.

**Results:** In vitro assays showed that MB-Pro has more efficient photodynamic activities than MB alone for the colon cancer cells, owing to lysosome rupture causing the rapid necrotic cell death. In this study, we coupled protamine with MB for high efficacy PDT. The conjugates localized in the lysosomes and enhanced the efficiency of PDT by inducing necrotic cell death, whereas PDT with non-coupled MB resulted in only apoptotic processes.

**Discussion:** Our research aimed to enhance PDT by engineering the photosensitizers using CPPs coupled with methylene blue (MB). MB alone permeates through the cell membrane and distributes into the cytoplasm, whereas coupling of MB dye with CPPs localizes the MB through an endocytic mechanism to a specific organelle where the localized conjugates enhance the generation of reactive oxygen species (ROS) and induce cell damage.

**Keywords:** methylene blue, protamine, CPP, photodynamic therapy, bioconjugation, anticancer, fluorescent

Correspondence: Yong Ho Kim  
School of Materials Science & Engineering,  
Gachon Pain Center and Department of  
Physiology, College of Medicine, Gachon  
University, Incheon 21999, Republic of  
Korea  
Tel +82-32-899-6691  
Fax +82-32-724-9071  
Email euro16@gachon.ac.kr

Hoonsung Cho  
School of Materials Science & Engineering,  
Chonnam National University, Gwangju  
61186, Republic of Korea  
Tel +82-62-530-1717  
Fax +82-62-530-1699  
Email cho.hoonsung@jnu.ac.kr

## Introduction

Photodynamic therapy (PDT) is a safe and effective strategy to destroy cancer cells; it is applicable in practically all cancer cell types, increases the specificity of chemo-medicinal treatments, and requires lower emission of energy than other treatments. PDT has been gradually exploited because of the lack of cumulative toxic effects and the simplicity of its procedures for use in outpatients.<sup>1</sup> PDT is an alternative to surgical resection for the treatment of colon cancer as it is practicable and does not affect the healing of a cross-connection between adjacent channels.<sup>2</sup>

The efficacy of PDT is determined by three components: light, a photosensitizer, and oxygen.<sup>3</sup> An ideal photosensitizer should meet several criteria, including

chemical purity, tumor specificity, rapid accumulation in target tissues or organs, rapid clearance, activation at wavelengths that penetrate deep inside tissues, ability to induce tissue damage when activated by high potential light, and no toxicity without photoactivation.<sup>4</sup>

The photosensitizer absorbs energy directly from a specific light source, which it then transfers to molecular oxygen to generate reactive oxygen species (ROS) and that makes singlet oxygen<sup>1,2</sup>. The singlet oxygen is particularly electrophilic and can oxidize electron-rich double bonds in macro-scale molecules.<sup>5</sup> It is the main cytotoxic product of PDT.<sup>6</sup> The primary targets of the singlet oxygen in the cells are the double bonds that constitute allylic hydroperoxides.<sup>7,8</sup> Lipid peroxidation in the cell membranes has been associated with several cell processes, including increases in ion permeability, reductions in membrane fluidity, and cross-linking or deactivation of membrane proteins.<sup>9</sup> PDT-induced cell death occurs by two mechanisms: apoptosis or necrosis. Apoptosis from PDT is initiated by an intra- or extra-

cellular signal that activates caspase and initiates DNA fragmentation. In apoptosis, the cell shrinks, the nuclear chromatin undergoes pyknosis, and the nucleus is dispersed into apoptotic bodies. Necrosis, on the other hand, commonly proceeds via damage to cellular ion homeostasis, which causes water influx and a loss of membrane integrity.<sup>10,11</sup>

Methylene blue (MB) is a near-infrared dye that has the absorption peak around a wavelength of 665 nm and fluorescence peak around a wavelength of 685 nm.<sup>12</sup> In this study, we used MB for a photosensitizer and MB simulated by light activation can produce a variety of reactive oxygen species (ROS) through type I and type II reactions, including singlet oxygen molecules,<sup>1</sup>  $O_2$  superoxide anion radicals,<sup>1</sup>  $O_2^-$  and hydroxyl radicals (OH.) in Figure 1.<sup>13</sup> MB interacts preferentially with negatively charged interfaces and produces some ROS, including hydroxyl radicals, through the Fenton reaction.<sup>14,15</sup> MB has also been used as a fluorescence marker for organelle localization.<sup>13</sup>

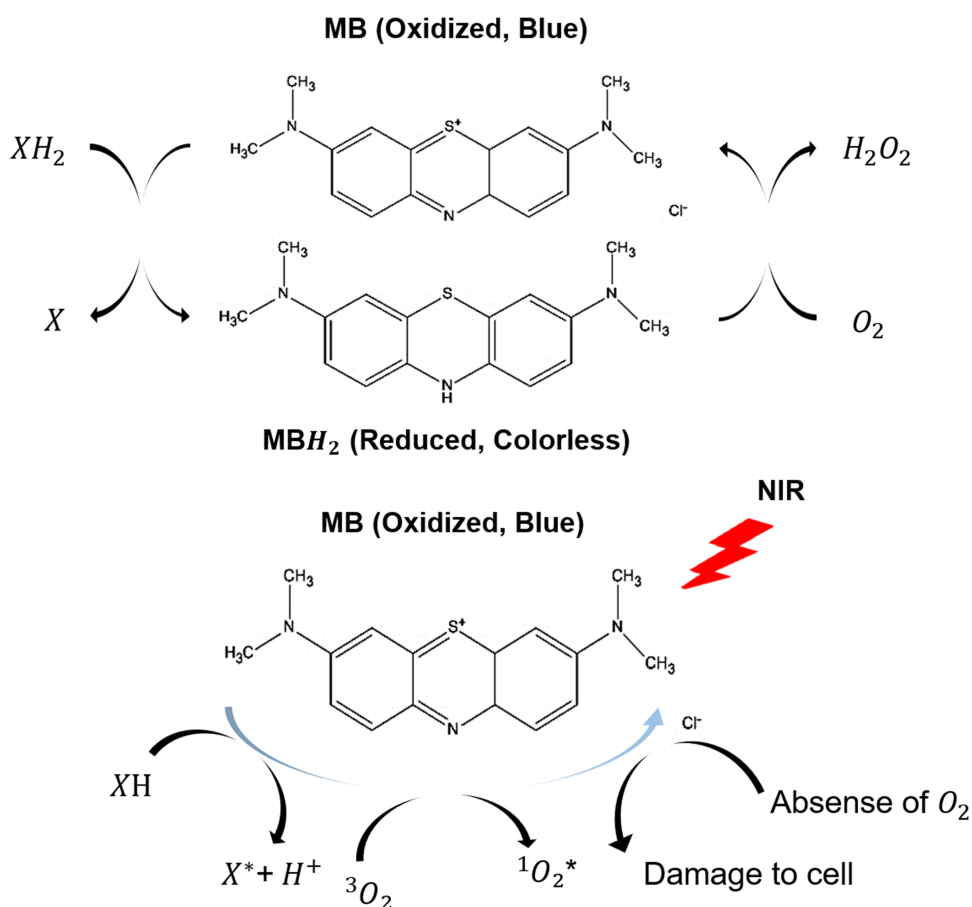


**Figure 1** Mechanism of Methylene blue reduction produce hydrogen peroxide and photodynamic therapy in methylene blue shows production ROS which induces cell damages.

The electric potential in the cells can vary greatly, from the slightly negative potential of the cytoplasmic membrane to the highly negatively charged internal mitochondrial membrane and polyelectrolytes (nucleic acids and polysaccharides).<sup>16,17</sup> Positively charged photosensitizers centralize in the mitochondria, owing to the high negative charge in this organelle.<sup>18</sup> MB actively interacts with these organelles; moreover, MB for use in PDT acts directly on negatively charged membranes and electrolytes.<sup>19</sup>

MB was able to enter the cytoplasm and then can localize in various subcellular structures and damage them on near-infrared light.<sup>12</sup> So, MB induces ROS production by PDT cytoplasm or near the mitochondria, which has been shown to cause apoptosis.<sup>20,21</sup>

CPPs (cell-penetrating peptides) can enter the cytoplasm of cells and have been used for the directed endocytosis of biomolecules using CPP-biomolecule conjugates.<sup>22</sup>

Therefore, in this study, we synthesized MB with clinical-grade protamine, which belongs to the class of CPPs. Protamine is primarily used to neutralize the anticoagulant drug heparin. It consists of four similar arginine-rich peptides with membrane-translocating and nuclear-localizing actions.<sup>23</sup>

CPPs may help deliver protein cargos directly to endosomes and lysosomes for therapeutic effects on the target organelles.<sup>24</sup>

The prior study found that lysosomes, the organelles containing numerous hydrolases, that release lysosomal proteases, thus leading to cell necrosis.<sup>25</sup>

Photosensitizers encapsulated in protamine cages can enter tumor cells and generate singlet oxygen for photodynamic therapy (PDT). Our goal was to couple protamine with MB. The conjugates of MB and protamine (MB-Pro) are preferentially internalized to the lysosomes where they exhibit lysosomal injury-inducing necrosis.<sup>26–28</sup>

This study explains the conjugation of Methylene Blue and clinical Protamine and the localization of the conjugates to lysosome by endocytosis. The conjugation provides the enhanced phototoxicity on MB. We describe the mechanistic molecular analysis of the *in vitro* assay and new applications for the conjugation of CPPs for the imaging and treatment of cancer.

## Materials and Methods

### Reagents and Materials

Unless otherwise stated, all chemicals were supplied by Sigma Aldrich Co. (St. Louis, MO, USA). HT-29 colorectal

adenocarcinoma cells were obtained from the American Type Culture Collection (ATCC, Manassas, VA, USA). The following kits and reagents were used in the experimental protocols: McCoy's 5A Medium Modified (Welgene Co., No. LM 005–02), MonocarboxyMethylene Blue Succinimidyl Ester (MB, BIOSEARCH Technologies, No. 113414), fetal bovine serum (FBS; Thermo Fisher Scientific, No. 16000044), DMSO anhydrous (Life Technologies Co, No. LOT. 0305C186), penicillin-streptomycin (Life Technologies, No. 15140122), trypsin-EDTA (Welgene Co, No. LS 015–10), LysoTracker Green (Thermo Fisher Scientific, No. L7526), protamine sulfate (Hanlim Pharmaceutical Co, No. 339, MW=4.1 kDa), AKTA Prime plus Fast Protein Liquid Chromatography (FPLC; GE Healthcare Lifesciences, USA), and EZ-Cytox (Dogenbio Co., Korea).

### Synthesis of MB-Pro

MB-Pro was synthesized by mixing 417  $\mu$ L of methylene blue solution (10 mM in DMSO) with 342  $\mu$ L of protamine sulfate (2.439 mM) and an additional 1 mL 1X phosphate buffered saline (PBS) for a total ratio of Pro: MB of 1:5. The pH was adjusted to 8.5 by adding sodium carbonate buffer with magnetic stirring. The reaction was carried out in a vial at 27°C for 4 h. The product was stored at 4°C until purification.

### Purification of MB-Pro

The MB-Pro mixture was purified by FPLC using two HiTrap Desalting columns with Sephadex G-25 Superfine size exclusion medium from GE Healthcare. Prior to separation, the column was wet with PBS. The purification was performed on AKTA Prime plus at room temperature while monitoring conductivity and UV. The gradient flow rate in the column was about 1 mL/min, and 0.3 mL fractions were collected upon the injection of the conjugated sample. Following purification, we used time-of-flight mass spectrometry (MALDI-TOF-MS) for the identification of and differentiation between the MB, Pro, and MB-Pro fractions.

### Cellular Uptake of MB-Pro and MB

Cellular uptake was assessed by fluorescence microscopy. HT-29 cells were seeded in a confocal dish and incubated at 37°C. After 1 day, 10  $\mu$ M of MB-Pro or MB was added to the culture medium and after 1 h 30 min, the cells were washed three times with PBS and resuspended in fresh media. To determine the localization of MB or MB-Pro,

the cells were incubated with 50 nM of LysoTracker (a green fluorescent dye that preferentially stains lysosomes) for 30 min. The cells with LysoTracker were also imaged after light irradiation to assess lysosomal rupture by PDT. After incubation with the dye, the cells were washed three times with PBS and resuspended in fresh media. Images were taken using Nikon inverted microscope eclipse DS-Ri2, Qi2 (Ex/Em, 665 nm/685 nm; exposure time, 30s).

## Photodynamic Treatment Assay

The HT-29 cells were seeded in 96-well plates and incubated with MB-Pro or MB (10  $\mu$ M) for 2 h at 37°C. After washing with PBS, the media was replaced, and the cells were irradiated with a narrow band filter covering the entire area of each well. The power source was an OSL2 (Thorlabs) with a 0.065 W halogen lamp, and radiation energy was gauged with a PM100D optical power and energy meter (Thorlabs).<sup>29</sup> The light passed through a 540/550 nm single-band filter (Semrock) and each well bottom of the 96-well plates (0.3 cm<sup>2</sup>) was exposed to the light for various times, resulting in an irradiation energy of 15 J/cm<sup>2</sup>, 30 J/cm<sup>2</sup> and 60 J/cm<sup>2</sup>. As controls, we included cells not exposed to the photosensitizer, not exposed to the light, or not exposed to either the photosensitizer or the light. All experiments were repeated three times.

## In vitro Cytotoxicity Assay

To evaluate the cytotoxicity of PDT using MB-Pro and MB, the cells were incubated for up to 3 days at 37°C in 5% CO<sub>2</sub> following PDT. Then, 10  $\mu$ L of EZ-Cyttox was added to each well, and the plates were incubated for 2 h at 37°C in the dark. Cells were then exposed to a digital orbital shaker (Scilab Instruments Co, No. SSO-2D) at 200 rpm. Absorption was subsequently measured at 450 nm on a microplate reader (Thermo scientific, Varioskan™ LUX multimode).

## Results and Discussion

### Coupling and Characterization of MB-Pro

The coupling of clinical protamine and MB is based on a solution-phase reaction that takes place at the N-terminal proline of protamine, resulting in complete modification of the protamine peptides. Protamine contains arginine-rich peptides, each with a unique reactive amine at the N-terminal proline; this structure enables control of the ratio of conjugation between protamine and MB.<sup>29</sup> As indicated in Figure 2A, the NHS ester of MB was reacted

with protamine to create the conjugate, and purification was performed by FPLC to eliminate any unreacted MB and protamine. Each fraction peak in Figure 2B shows the clear separation of conjugation reaction products by FPLC. MB-Pro, which has the highest molecular mass, extruded early, followed by protamine and MB, based on their respective molecular masses. Figure 2C shows the absorbance spectra of the eluates corresponding to each peak in Figure 2B, confirming the conjugation and purification of MB-Pro. The MB-Pro absorbance peaks reflected a combination of the absorbance peaks for pure protamine and pure MB, implying that MB-Pro has the properties of both MB and protamine (data not shown). Figure 2D and E show the MALDI-TOF data confirming (d) protamine (MW  $\approx$  4400 Da) mass and (e) the MB-Pro conjugate (MW  $\approx$  4900 Da) mass.

### Uptake Images of MB and MB-Pro

The HT-29 cells were incubated with both MB and MB-Pro in media for 2 h prior to fluorescence imaging. Images of both MB and MB-Pro in the cells were obtained simultaneously in an oil-merged lens system. Meanwhile, cell viability after imaging was not changed. Figure 3A shows HT-29 cells incubated with MB. MB permeated the cell membrane and localized in the mitochondria and organelles as well as the nucleus. Figure 3B shows a different pattern of MB-Pro staining in the cells. Fluorescent spots were localized in HT-29 cells stained with MB-Pro, implying that MB-Pro was internalized by endocytosis and accumulated in the lysosomes.<sup>29</sup>

### Lysosomal Localization of MB-Pro and Rupture Imaging by PDT

MB has been shown to enter the matrix and actively engage the mitochondria.<sup>19</sup> However, the conjugate MB-Pro was localized to specific subcellular compartments. To determine the sites of MB-Pro localization, we co-stained cells with the lysosomal targeting dye, LysoTracker, to verify lysosomal localization of MB-Pro (Figure 4).

Figure 4A shows co-staining images with a lysosomal marker and MB-Pro where, in some cases, the signal of MB-Pro overlaps with LysoTracker spots. Merged images appeared to imply that MB-Pro was localized in the lysosomes (yellow color). Figure 4B shows the cell with MB-Pro after PDT irradiation. Compared with the vivid spots observed in (b), the fluorescent signals of LysoTracker are dim and diffuse into the cytoplasm,

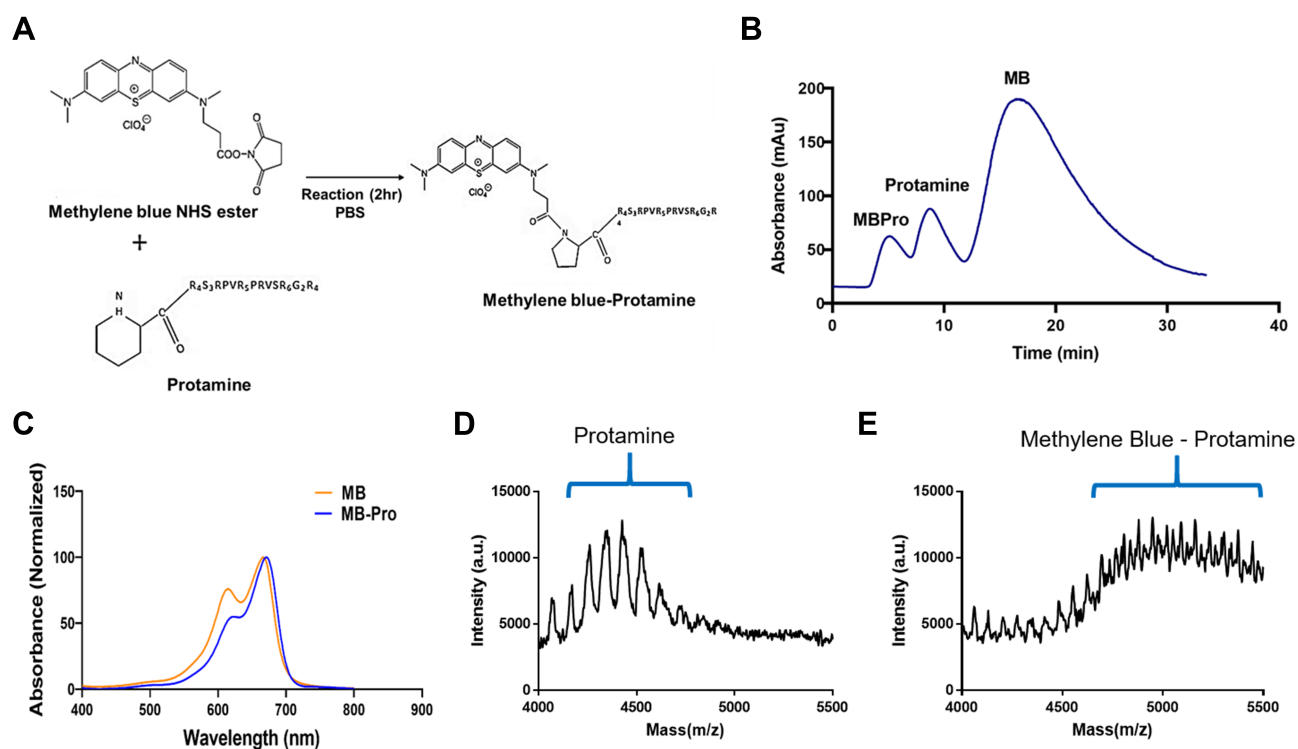


**Figure 2** (A) Synthesis of methylene blue-protamine (MB-Pro). The NHS ester of methylene blue reacts with the N-terminal proline of protamine to yield methylene blue-protamine. (B) FPLC data showed three fraction peaks equivalent to MB-Pro, protamine, and MB. (C) Absorbance spectra of MB-Pro and MB. (D and E) MALDI-TOF data showing protamine and the conjugation of methylene blue with protamine.

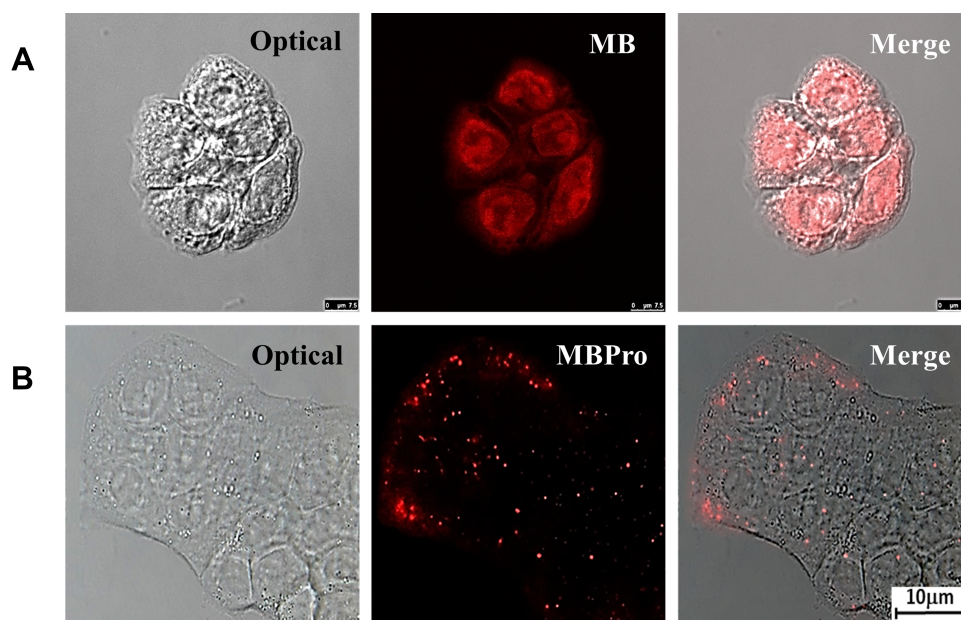


**Figure 3** Uptake images of HT-29 cells stained with (A) methylene blue and (B) methylene blue-protamine conjugates. Membrane-permeable MB stained throughout the cytoplasm (A), whereas the conjugate of MB and protamine was internalized by endocytosis and localized in the lysosomes (B).

indicating rupture of the lysosomes. Lysosomal rupture is known to result in the activation of necrotic death by causing water influx and a loss of membrane

integrity.<sup>10,11</sup> Furthermore, lysosomal rupture following MB-Pro treatment releases the photosensitizer from the organelles to other cellular compartments.

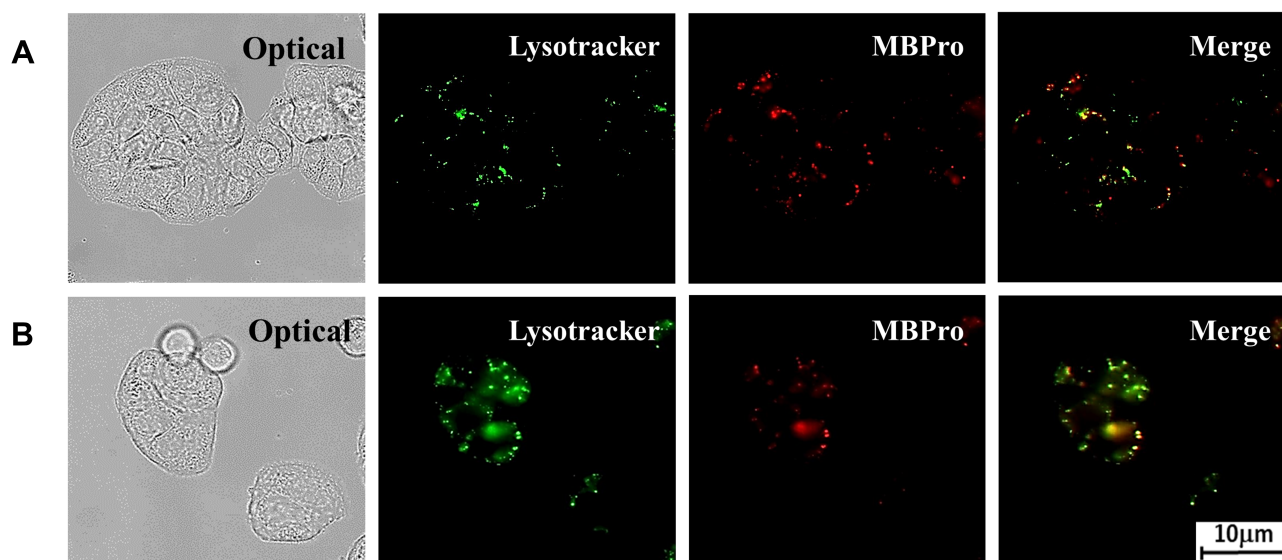


**Figure 4** Uptake images of co-staining with a lysosomal marker, Lysotracker, and MB-Pro in HT-29 cells. The intracellular endosomal localization of MB-Pro in lysosomes is shown in (A, B) shows the diffused fluorescent signals indicate lysosomal rupture by PDT.

## In vitro Cytotoxicity Assay

Cell viability was tested up to 3 days after PDT in HT-29 cells using the MTT assay. The wavelength of the radiation source for PDT was 540/550 nm, selected by a single-band filter. The wavelength was selected based on the maximum absorbance of the photosensitizer, MB. Firstly, we evaluated the effect of the concentration of photosensitizer on cell death. PDT was performed once with an irradiation energy of 30 J/cm<sup>2</sup>. Cells were then incubated for 2 days (Figure 5A) or 3 days (Figure 5B). As shown in Figure 5A), treatment with 1µM MB or MB-Pro and activation by laser light at 30 J/cm<sup>2</sup> did not result in any cell cytotoxicity compared to the control group (0 µM, laser 30 J/cm<sup>2</sup>). As the concentration of

the photosensitizer increased, cell viabilities decreased following activation by a light dose of 30 J/cm<sup>2</sup>; the values were minimal when cells were treated with 10 µM MB or MB-Pro. The viability of the cells treated with 10 µM MB and PDT or 10 µM MB-Pro and PDT was 80.8% and 81.5% after 2-day incubation, respectively. The significant differences of the cytotoxicity between MB-PDT and MB-Pro-PDT in 2 days are not shown. However, in 3 days after PDT, cell viability was significantly reduced. Viability was 75.5% in the MB-PDT group and 52.6% in the MB-Pro-PDT group. The cytotoxicity of MB-PDT increased by 5.3% between days 2 and 3 of incubation; however, the cytotoxicity of MB-Pro-PDT increased by 28.9% between days 2 and

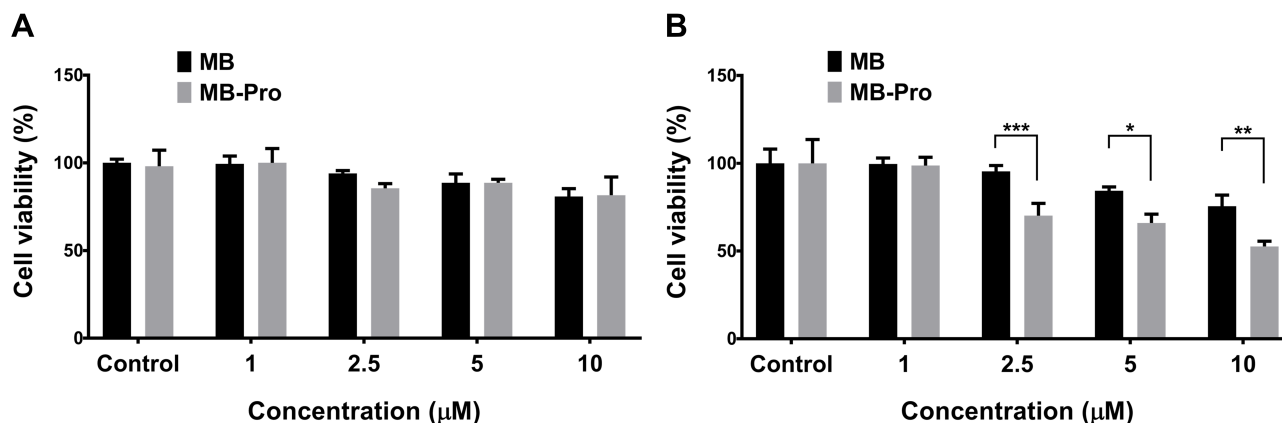


**Figure 5** Effect of different concentrations of both MB-Pro and MB on cell viabilities using the same irradiation energy at a time and incubating cells for 2 days (A) or 3 days (B) after PDT (n=5). The significant differences are shown as \* $P < 0.05$ , \*\* $P < 0.01$ , and \*\*\* $P < 0.001$ .

3. The efficiency of PDT was therefore significantly increased by MB-Pro. The difference between the cytotoxicity of MB and MB-Pro after 3 days was 22.9% at 10  $\mu\text{M}$  ( $P<0.01$ ).

Secondly, we measured the efficiency of PDT at different light energies with constant photosensitizer (MB and MB-Pro) concentrations. The cells were incubated post-treatment for 2 days (Figure 6A) or 3 days (Figure 6B). The dark control (MB 10  $\mu\text{M}$ , laser light 0  $\text{J}/\text{cm}^2$ ) exhibited no significant cell death after treatment with 10  $\mu\text{M}$  for MB and MB-Pro compared with the negative control subgroup (MB 0  $\mu\text{M}$ ). Increasing either the input energy or the incubation time increased the efficiency of PDT with both MB and MB-Pro. The significant differences of the cytotoxicity between MB-PDT and MB-Pro-PDT in 2 and 3 days are shown in Figure 6. Significant effects of PDT using MB-Pro were also observed after treatment with 60  $\text{J}/\text{cm}^2$  as shown in Figure 6B. The cell viability of PDT with MB-Pro was 32.2% at 10  $\mu\text{M}$  following 3 days of incubation and 72.3% by PDT with MB alone when using an irradiation energy of 60  $\text{J}/\text{cm}^2$ ; the difference in cell viabilities for MB and MB-Pro was 40% ( $P<0.001$ ). PDT using MB did not exceed 30% cytotoxicity; however, PDT with MB-Pro resulted in almost 70% cytotoxicity.

In another study, no meaningful distinction in cell viability was found between treatments with 10 or 15  $\mu\text{M}$  of MB in the MB-PDT group. This implies that increasing the concentration of MB higher than 10  $\mu\text{M}$  for MB-PDT does not increase the efficacy of MB-PDT.<sup>30</sup> Thus, the application of 10  $\mu\text{M}$  MB-Pro with 60  $\text{J}/\text{cm}^2$  laser irradiation is optimal for causing cell

death in PDT, as opposed to non-conjugated MB treatment.

## PDT Effect on Cell Death in Response to MB-Pro and MB

Several studies have reported photodynamic cell death mediated by MB as measured by flow cytometry and fluorescence microscopy. Some studies have shown that, in cells incubated with MB, MB entered the cytoplasmic matrix and actively bound to the mitochondria.<sup>13</sup> The bound MB generated singlet oxygen in the mitochondria following PDT, causing rapid mitochondrial permeabilization of the inner membrane and release of cytochrome C.<sup>31</sup> Therefore, MB-based PDT inhibits mitochondrial function. Release of cytochrome C activated caspase 9, which subsequently activated the caspase effector factor caspase 3.<sup>30</sup>

Thus, we suggest that activation of MB by PDT causes cell destruction through the mitochondria, where release of cytochrome C from the mitochondria triggers caspase 9, caspase 3, and some poly (ADP-ribose) polymerase (PARP) proteins to induce cell apoptosis. Only a minute amount of selective lysosomal damage is associated with the induction of apoptosis.<sup>32</sup> In contrast, activation of MB-Pro by PDT disrupts lysosome function, resulting in necrosis (Figure 7). Necrosis by PDT with MB-Pro was visualized in time-lapse confocal experiments (Supplementary data video 1) showing bleb and disruption of the membrane. For visualization of the necrosis by PDT, time-lapse experiments were performed. The images were taken at 30-s intervals for 1 h using LSM 510 confocal microscope and the images were made to a video. Confocal excitation lasers were used as an irradiation source.

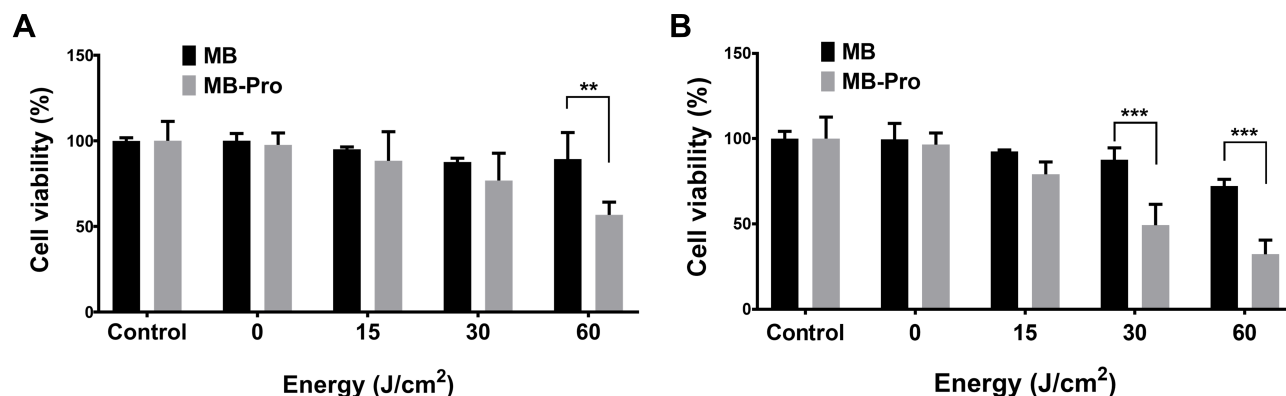


**Figure 6** Effect of different irradiation energy on cell viability using the same concentration for both MB-Pro and MB ( $n=5$ ). Cells were incubated for 2 days (A) and 3 days (B) after PDT, respectively. The significant differences are shown as  $**P<0.05$ , and  $***P<0.001$ .

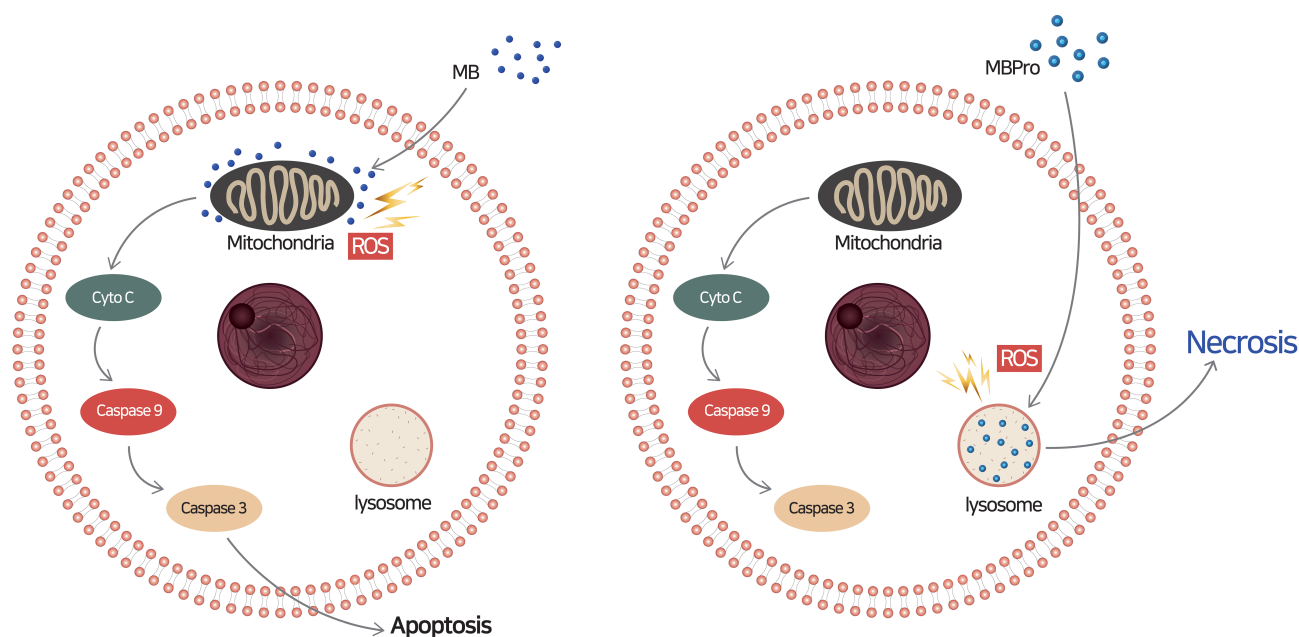


**Figure 7** Mechanism of action of PDT by MB and MB-Pro localized in the mitochondria and lysosome, respectively. MB penetrates into the mitochondria releasing cytochrome C, triggering caspase 9 and caspase 3 to induce cell apoptosis (left). MB-Pro penetrates the lysosome causing necrosis (right).

## Conclusion

Most cell-permeable photosensitizers localize in the cytoplasm. As shown in this study, MB is one of these drugs, localized in the cytoplasm as well as nearby organelles, including the mitochondria.

Traditionally, lysosomes have not been considered intracellular targets for photo-oxidants. However, in this study, we showed that the photo-damage by photosensitizers can occur in the lysosome using photosensitizers coupled with CPPs, resulting in more efficient PDT than the photo-damage caused by photosensitizers which internalized in the cytoplasm.

MB-Pro preferentially localized to the lysosome; this strategy could be applied to fluorescence imaging contrast agents and cell-specific targeting ligands. Our approach using a conjugate of protamine and MB provides new opportunities for utilizing multifunctional nanomaterials for the fluorescent imaging and the cancer therapy.

## Funding

This study was supported by Basic Science Research Program through the National Research Foundation of Korea (NRF) funded by the Ministry of Education (2018R1D1A1B07049867 and 2018R1D1A1B07049089).

## Disclosure

The authors report no conflicts of interest in this work.

## References

1. Van Hillegerberg R, Hekking-Weijma J, Wilson J, Edixhoven-Bosdijk A, Kort W. Adjuvant intraoperative photodynamic therapy diminishes the rate of local recurrence in a rat mammary tumour model. *Br J Cancer*. 1995;71(4):733. doi:10.1038/bjc.1995.143
2. Haddad R, Kaplan O, Brazovski E, et al. Effect of photodynamic therapy on normal fibroblasts and colon anastomotic healing in mice. *J Gastrointest Surg*. 1999;3(6):602–606. doi:10.1016/S1091-255X(99)80081-X
3. Leite IS, Geralde MC, Salina AC, et al. Near-infrared photodynamic inactivation of *S. pneumoniae* and its interaction with RAW 264.7 macrophages. *J Biophoton*. 2018;11(1):e201600283. doi:10.1002/jbio.201600283
4. Jori G. Tumour photosensitizers: approaches to enhance the selectivity and efficiency of photodynamic therapy. *J Photochem Photobiol B*. 1996;36(2):87–93. doi:10.1016/S1011-1344(96)07352-6
5. Verma SK, Jha E, Panda PK, et al. Molecular insights to alkaline based bio-fabrication of silver nanoparticles for inverse cytotoxicity and enhanced antibacterial activity. *Mater Sci Eng*. 2018;92:807–818. doi:10.1016/j.msec.2018.07.037
6. Ochsner M. Photophysical and photobiological processes in the photodynamic therapy of tumours. *J Photochem Photobiol B*. 1997;39(1):1–18. doi:10.1016/S1011-1344(96)07428-3
7. Lamola A, Yamane T, Trozzolo A. Cholesterol hydroperoxide formation in red cell membranes and photohemolysis in erythropoietic protoporphyria. *Science*. 1973;179(4078):1131–1133. doi:10.1126/science.179.4078.1131
8. Doleiden F, Fahrenholtz S, Lamola A, Trozzolo A. Reactivity of cholesterol and some fatty acids toward singlet oxygen. *Photochem Photobiol*. 1974;20(6):519–521. doi:10.1111/j.1751-1097.1974.tb06613.x
9. Girotti AW. Photodynamic lipid peroxidation in biological systems. *Photochem Photobiol*. 1990;51(4):497–509. doi:10.1111/j.1751-1097.1990.tb01744.x
10. Plaetzer K, Kiesslich T, Oberdanner CB, Krammer B. Apoptosis following photodynamic tumor therapy: induction, mechanisms and detection. *Curr Pharm Des*. 2005;11(9):1151–1165. doi:10.2174/1381612053507648



11. Lemasters JJ. Dying a thousand deaths: redundant pathways from different organelles to apoptosis and necrosis. *Gastroenterology*. 2005;129(1):351–360. doi:10.1053/j.gastro.2005.06.006
12. Tuite EM, Kelly JM. New trends in photobiology: photochemical interactions of methylene blue and analogues with DNA and other biological substrates. *J Photochem Photobiol B*. 1993;21(2):103–124. doi:10.1016/1011-1344(93)80173-7
13. Tardivo JP, Del Giglio A, De Oliveira CS, et al. Methylene blue in photodynamic therapy: from basic mechanisms to clinical applications. *Photodiagnosis Photodyn Ther*. 2005;2(3):175–191. doi:10.1016/S1572-1000(05)00097-9
14. Junqueira HC, Severino D, Dias LG, Gugliotti MS, Baptista MS. Modulation of methylene blue photochemical properties based on adsorption at aqueous micelle interfaces. *PCCP*. 2002;4(11):2320–2328. doi:10.1039/b109753a
15. Severino D, Junqueira HC, Gugliotti M, Gabrielli DS, Baptista MS. Influence of negatively charged interfaces on the ground and excited state properties of methylene blue. *Photochem Photobiol*. 2003;77(5):459–468. doi:10.1562/0031-8655(2003)077<0459:IONCIO>2.0.CO;2
16. Voet D, Voet J. *Biochemistry*. 2nd ed. New York: John Wiley and Sons. Inc; 1995:850–861.
17. Baptista M. Supramolecular assemblies of natural and synthetic polyelectrolytes. *Handbook Polyelectrolyte Appl*. 2002;1:165–181.
18. Kandela IK, Bartlett JA, Indig GL. Effect of molecular structure on the selective phototoxicity of triarylmethane dyes towards tumor cells. *Photochem Photobiol Sci*. 2002;1(5):309–314. doi:10.1039/b110572h
19. Gabrielli D, Belisle E, Severino D, Kowaltowski A, Baptista M. Binding, aggregation and photochemical properties of methylene blue in mitochondrial suspensions. *Photochem Photobiol*. 2004;79:227–232. doi:10.1562/BE-03-27.1
20. Stewart F, Baas P, Star W. What does photodynamic therapy have to offer radiation oncologists (or their cancer patients)? *Radiother Oncol*. 1998;48(3):233–248. doi:10.1016/S0167-8140(98)00063-2
21. Jiang C, Yang W, Wang C, et al. Methylene blue-mediated photodynamic therapy induces macrophage apoptosis via ROS and reduces bone resorption in periodontitis. *Oxid Med Cell Longev*. 2019;2019:1529520. doi:10.1155/2019/1529520
22. Richard JP, Melikov K, Vives E, et al. Cell-penetrating peptides: A reevaluation of the mechanism of cellular uptake. *J Biol Chem*. 2003;278(1):585–590. doi:10.1074/jbc.M209548200
23. Reynolds F, Weissleder R, Josephson L. Protamine as an efficient membrane-translocating peptide. *Bioconjug Chem*. 2005;16(5):1240–1245. doi:10.1021/bc0501451
24. Maxfield FR. Role of endosomes and lysosomes in human disease. *Cold Spring Harb Perspect Biol*. 2014;6(5):a016931. doi:10.1101/cshperspect.a016931
25. Kroemer G, Jaattela M. Lysosomes and autophagy in cell death control. *Nat Rev Cancer*. 2005;5:886–897. doi:10.1038/nrc1738
26. Castano AP, Demidova TN, Hamblin MR. Mechanisms in photodynamic therapy: part one—photosensitizers, photochemistry and cellular localization. *Photodiagnosis Photodyn Ther*. 2004;1(4):279–293. doi:10.1016/S1572-1000(05)00007-4
27. Garg AD, Maes H, Romano E, Agostinis P. Autophagy, a major adaptation pathway shaping cancer cell death and anticancer immunity responses following photodynamic therapy. *Photochem Photobiol Sci*. 2015;14(8):1410–1424. doi:10.1039/C4PP00466C
28. Oleinick NL, Evans HH. The photobiology of photodynamic therapy: cellular targets and mechanisms. *Radiat Res*. 1998;150(5s):S146–S156. doi:10.2307/3579816
29. Park C-K, Kim YH, Hwangbo S, Cho H. Photodynamic therapy by conjugation of cell-penetrating peptide with fluorochrome. *Int J Nanomedicine*. 2017;12:8185. doi:10.2147/IJN.S148332
30. Jiang C, Yang W, Wang C, et al. Methylene blue-mediated photodynamic therapy induces macrophage apoptosis via ROS and reduces bone resorption in Periodontitis. *Oxid Med Cell Longev*. 2019;1529520.
31. Cai J, Yang J, Jones D. Mitochondrial control of apoptosis: the role of cytochrome c. *Biochimica et Biophysica Acta (BBA) Bioenerg*. 1998;1366(1):139–149. doi:10.1016/S0005-2728(98)00109-1
32. Guicciardi ME, Leist M, Gores GJ. Lysosomes in cell death. *Oncogene*. 2004;23(16):2881–2890. doi:10.1038/sj.onc.1207512

## International Journal of Nanomedicine

### Publish your work in this journal

The International Journal of Nanomedicine is an international, peer-reviewed journal focusing on the application of nanotechnology in diagnostics, therapeutics, and drug delivery systems throughout the biomedical field. This journal is indexed on PubMed Central, MedLine, CAS, SciSearch®, Current Contents®/Clinical Medicine,

Journal Citation Reports/Science Edition, EMBase, Scopus and the Elsevier Bibliographic databases. The manuscript management system is completely online and includes a very quick and fair peer-review system, which is all easy to use. Visit <http://www.dovepress.com/testimonials.php> to read real quotes from published authors.

Submit your manuscript here: <https://www.dovepress.com/international-journal-of-nanomedicine-journal>